Journal of Mining and Environment (JME), Vol. 14, No. 4, 2023, 1141-1153

Shahrood University of Technology

Journal of Mining and Environment (JME)

Journal homepage: www.jme.shahroodut.ac.ir

Iranian Society of Mining Engineering (IRSME)

Soil Liquefaction Susceptibility of Akcay Residential Area (Biga Peninsula, Turkey) Close to North Anatolian Fault Zone

Sener Ceryan[1], Pijush Samui[2], Osman Samed Ozkan[3], Samet Berber[1], Sule Tudes[4], Hakan Elci[5]*, and Nurcihan Ceryan[6]

1. Department of Geological Engineering, Balikesir University, Balikesir, Turkey
2. Department of Civil Engineering, NIT Patna, Patna, Bihar, India
3. Graduate School of Natural and Applied Sciences, Balikesir University, Balikesir, Turkey
4. Department of City and Regional Planning, Faculty of Architecture Gazi University, Ankara Turkey
5. Torbalı Vocational School, Dokuz Eylul University, Izmir, Turkey
6. Department of Mining and Mineral Extraction, Balikesir Vocational School, Balikesir University, Balikesir, Turkey

Article Info

Received 18 May 2023
Received in Revised form 17 June 2023
Accepted 28 June 2023
Published online 28 June 2023

DOI: 10.22044/jme.2023.13145.2395

Keywords

North Anatolian Fault Zone
Soil Liquefaction
Liquefaction Potential Index
Liquefaction Severity Index

Abstract

Balikesir province Akcay district (Biga Peninsula, South Marmara Region, Turkey); the studied area is located on the southern branch of the North Anatolian Fault Zone, where some earthquake, 1867 Edremit (Mw =7.0), 1919 Ayvalik-Sarmisakli (Mw = 7.0), 1944 Edremit (Mw =6.4) and 1953 Yenice (Mw = 7.2) earthquakes occurred in the historical and the instrumental period. In the said area, generally, the groundwater level is high and sandy soils are widespread. In this study, therefore topography, depth of groundwater table and soil characteristics of the said area were investigated in terms of susceptibility to liquefaction. In addition, the safety factor against liquefaction (FL) for the soil layers were determined by using simple procedure based on SPT-N values. Then the spatial distributions of the safety factor at 3 m, 6 m, 9 m, 12 m, 15 m and 18 m depths were obtained. Taking into considering FL values obtained, the liquefaction potential index and the liquefaction severity index of soil profile in the location of boring were calculated, then the spatial distributions of these index were obtained. According to the maps obtained, 5.8% of the studied area has low liquefaction potential, 10.7% medium liquefaction potential, 18.3% high liquefaction potential, and 53.8% very high liquefaction potential, and 22.7% of the study area has very low liquefaction severity, 17.1% low liquefaction severity, 47.7% moderate liquefaction severity, and 1.1% high liquefaction severity and 11.4% of the studied area has none-liquefiable soil.

1. Introduction

The term “liquefaction” has been first used by Terzaghi and Peck (1948) [1] to describe the significant loss of strength of very loose sands causing flow failures due to slight disturbance. In its more general terms, liquefaction can be defined as the reduction of both shear strength and stiffness of saturated loose sandy soils due to excess pore pressure generation under cyclic loading [2].

Starting with 1964 Niigata (Japan) and Alaska Earthquakes (USA), seismic soil liquefaction behavior has become a major research stream in geo-technical earthquake engineering [3]. In the 1989 Loma Prieta earthquake [4], 1995 Great Hanshin earthquake [5], 1999 Chi-Chi earthquake [6], 1999 Kocaeli-Adapazri earthquake [7], Canterbury earthquake [8], 2018 Central Sulawesi earthquake [9], and 2023 Kahramanmaras earthquake (Turkey), liquefaction cause significant loss and damage to engineering structures.

Since soil liquefaction has contributed to devastating effects of earthquakes, investigators have started researching in order to evaluate the seismic induced soil liquefaction Seismic soil liquefaction triggering curves are first introduced by [10], Seed *et. al.*, (1984) on the basis of simplified procedure by Seed and Idriss (1971) [11]. There are several methods developed to evulation liquefaction triggering [12]. These methods are stress-based approaches [11], strain-based approaches [13], energy-based procedures

✉ *Corresponding author: hakan.elci@deu.edu.tr (H. Elci)*

[14], laboratory tests [15], computational mechanics-based methods [16], and field measurement of pore-pressure generation under dynamic loading [12].

Balikesir province Akcay district (Turkey) (Figure 1) is located on the southern coast of Edremit Gulf of Aegean Sea.

As is well known, Anatolian land (Turkey) has very complex tectonic features because of the motions of Arabian, African and Eurasian plates (see Figure 1). The Eurasian Plate is located north of the North Anatolian Fault. The Arabian Plate is under thrusting the Anatolian block in eastern Turkey, leading to the formation of high elevations and volcanism in Turkey. The African Plate is subducting beneath the Aegean Sea and central and western Turkey, creating the Aegean volcanic arc consisting of (from west to east) Methana, Milos, Santorini, and Nisyros. The motions of these plates create a number of single active faults and fault systems, which generated devastating earthquakes in the past, and also are capable to produce many significant earthquakes in the future. The North Anatolian Fault Zone (NAFZ), one of the major active tectonic features in Anatolia, have a 1500 km long with right-lateral strike-slip fault system. Since the Pliocene, the NAF forming the boundary between the Eurasian and Anatolian plates is blamed for the westward motion of the Anatolia with respect to Eurasia [17, 18]. Around the south of Duzce city, the approximately E-W trend of NAF turns into the NE direction, and NAF spits into two main subsections [18], (Figure 1). The northern branch is passing through the Sapanca-Kocaeli then it lies towards into the Marmara Sea. Two big earthquakes occurred at İzmit (Mw = 7.4) and Duzce (Mw = 7.2) in 1999 [18].

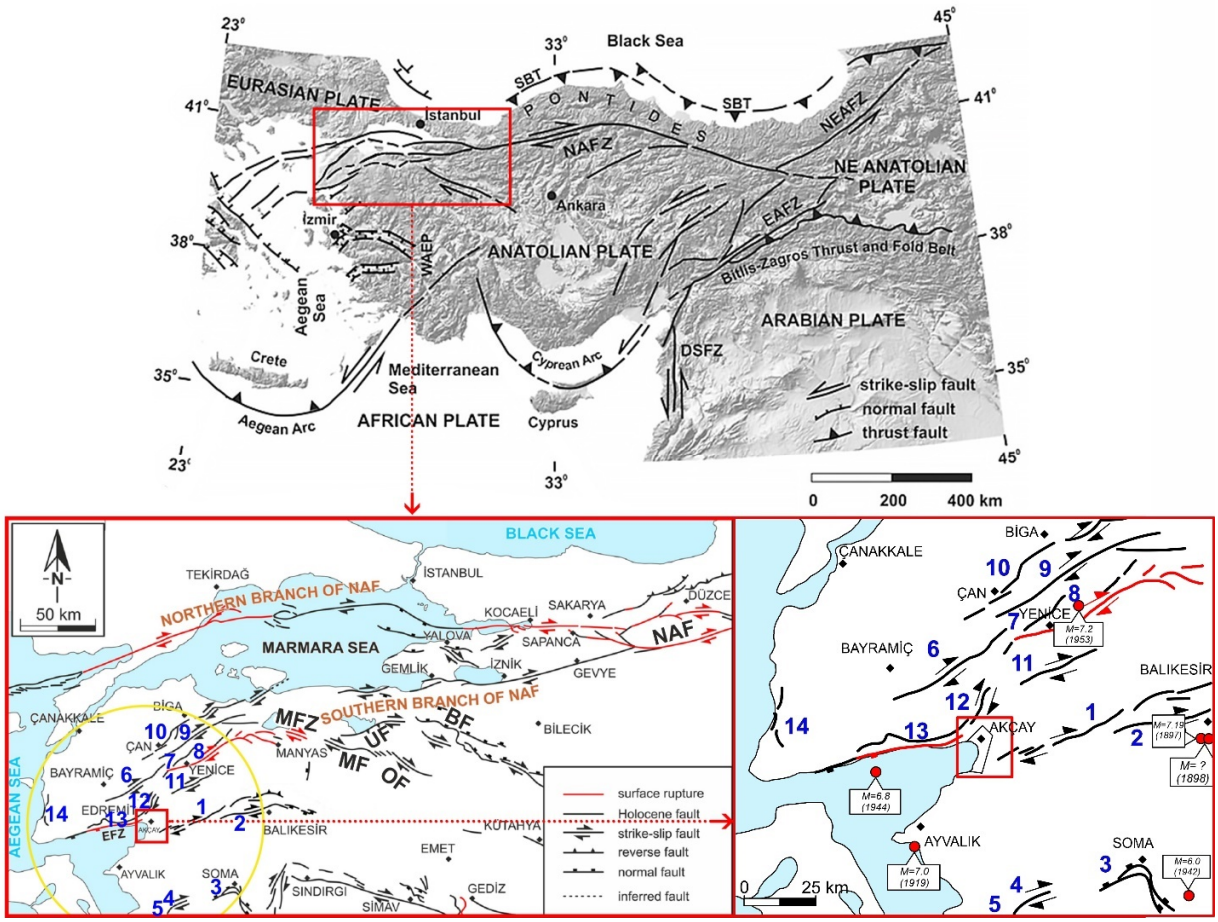

Figure 1. Simplified neotectonic map and relief of the region and the study area [17], Simplifed active fault map of Northwest Anatolia [18] and major earthquakes in the instrumental period affecting the study area (NAF, North Anatolian Fault; BF, Bursa Fault; UF, Ulubat Fault; MF, Mustafakemalpaşa Fault; OF, Orhangazi Fault; MFZ, Manyas Fault Zone; 1: Havran-Balya Fault, 2: Balikesir Fault, 3: Soma-Kırkagac Fault Zone, 4: Bergama fault, 5: Zeytindag Fault Zone, 6: Evciler fault, 7: Bekten Fault, 8: Yenice-Gonen Fault, 9: Sarikoy Fault, 10: Biga-Can Fault Zone, 11: Pazarkoy Fault, 12: Altınoluk segment of Edremit Fault Zone (EFZ), 13: Zeytinli segment of EFZ, 14: Kestanbol Fault)

The southern branch includes many parallel/subparallel dextral strike-slip faults all along the southern Marmara region [19]. These faults, located just north and west of the study area, are Eviler Fault, Bekciler Fault, Yenice–Gönen Fault, Sarikoy fault, Can Fault Zone, Pazarkoy Fault, and Edremit Fault Zone including Zeytinli and Altınoluk segments (Figure 1b). Between 160 and 1898 AD, 30 earthquakes were reported at the western termination of the southernbranch of the NAFZ, including the EFZ and the surrounding area in 18 locations [18, 20]. In the instrumental period, the southern branch generated Ayvalik-Sarmisakli (Mw = 7.2, [19], Edremit (Mw = 6.4) and Yenice (Mw = 7.2) earthquakes in 1919, 1944 and 1953 respectively [20].

The Havran- Balikesir Fault Zone (HBFZ located just south of Akcay is one of the seismically active main structures in the study area. According to the results of these paleo-seismological studies in this fault zone, the earthquakes occurred in 1897 and 1898 may have a magnitude of 7.19 degrees [18, 21].

The other two sources that will create an earthquake hazard for Akcay and its surroundings are the Kestanbul fault and Soma-Kırkağaç Fault zone to the south of the said area. These fault and fault zone are capable of generating an earthquake with a moment magnitude of 6.6-6.8. Two large earthquakes occurring in 1919 and 1942 are known to have caused damage and loss of life in the Soma-Kırkağaç (Manisa) region [22].

Akcay village, the studied area, is located on the southern branch of the North Anatolian Fault (NAF). In the same time, alluvial soil is widespread in the said area. For this reason, the liquefaction potential of this area, where the groundwater depth is low, was investigated. In this study, the liquefaction severity index map and the liquefaction potential map are produced. In order to obtain the safety factor against liquefaction of the alluvium soil layers in Akcay district e simplified method given in Youd et al., (2001), [23] was used. The approach given in the [24], Sonmez (2003) was used to produce the liquefaction potential map and the liquefaction severity index map of the said area was prepared based on Sonmez and Gokceoğlu (2005), [25].

2. Methodology

In this study, in the first step, the geological and the geo-technical data of the studied area were collected and analyzed. These data provided from the microzonation report, which is as a basis for development plan of Edremit (Balikesir) [26]. In this study, 152 drilling logs were used (Figure 2a). According to the results of the analysis topographic map, slope, underground water level map, the soil type map was created and spatial distributions of corrected SPT-N value at different depths in the studied area were determined. The classification of the soil samples was performed according to unified soil classification system given in the ASTM D2487-06 (2010) [27]. At the end of the said step, cyclic resistance ratio (CRR) of soil layer was calculated according to Youd *et al.,* (2001), [23].

In the second step, firstly, site-specific earthquake parameters such as the peak ground acceleration (a_{max}), the short-period map spectral acceleration coefficient (S_S) and map spectral acceleration coefficient for 1 s (S_1) for standard design earthquake ground motion level were identified from Turkish Earthquake Hazard Maps accessed through the website www.tdth.afad.gov.tr. The map spectral acceleration coefficients correspond to the geometric averages of the earthquake effects in two perpendicular horizontal directions. The said parameters were obtained by traditional probabilistic seismic hazard analyses. Within the Turkish Building Earthquake Code (2018), [28], earthquake ground motion spectrums are calculated for a 5% damping ratio based on reference soil conditions ($(Vs)_{50}$ = 760 m/s) for a certain level of earthquake ground motion. In this code, four different earthquake ground motion levels are defined. These are DD-I. DD-2. DD-3. and DD-4. Earthquake Ground Motion Level-2, DD-2, refers to the periodic earthquake ground motion, which has a 10% exceedance probability in 50 years, and the corresponding return period is 475 years. This ground motion is also called the standard design earthquake ground motion. And then the peak ground acceleration was obtained for the standard design earthquake ground motion. At the end of the said step, cyclic stress ratio (CSR) of soil layer was calculated according to Youd *et al.*, (2001), [23].

After calculating CRR and CSR, the factor of safety against liquefaction (F) was obtained, and then, considering this safety factor, the probability of liquefaction for soil layer (P_L) were calculated using the methods suggested by Juang *et al.*, (2003), [29].

In the last step, the liquefaction potential map and the liquefaction severity index map were created. For this, the approach given in the Sonmez (2003) [24] was used to obtained the liquefaction potential index of soil profile. And the liquefaction severity

index of soil profile was obtained based on Sonmez and Gokceoğlu (2005) [25]. The safety number of the soil layer against liquefaction was used in the calculation of the liquefaction potential index, and the probability of liquefaction was used in the calculation of the liquefaction severity index.

3. Topography, Depth of Groundwater Table and Soil Characteristics

The southwest border of the studied area reaches up to the Edremit Gulf coastline. Approximately 62% of the studied area is placed at about from 0 to 4 meters above sea level while %38 of the study area is placed at about from 4 to 15 meters above sea level (Figure 2b). The slope of 98 % of the studied area having less than 2 degrees (Figure 2c). In this studied area, the measurements of the elevation of groundwater table (GWT) were obtained between June and October 2016, when the rainfall is relatively low, and the map representing of the depth of groundwater table (GWT) was prepared (Figure 2d).

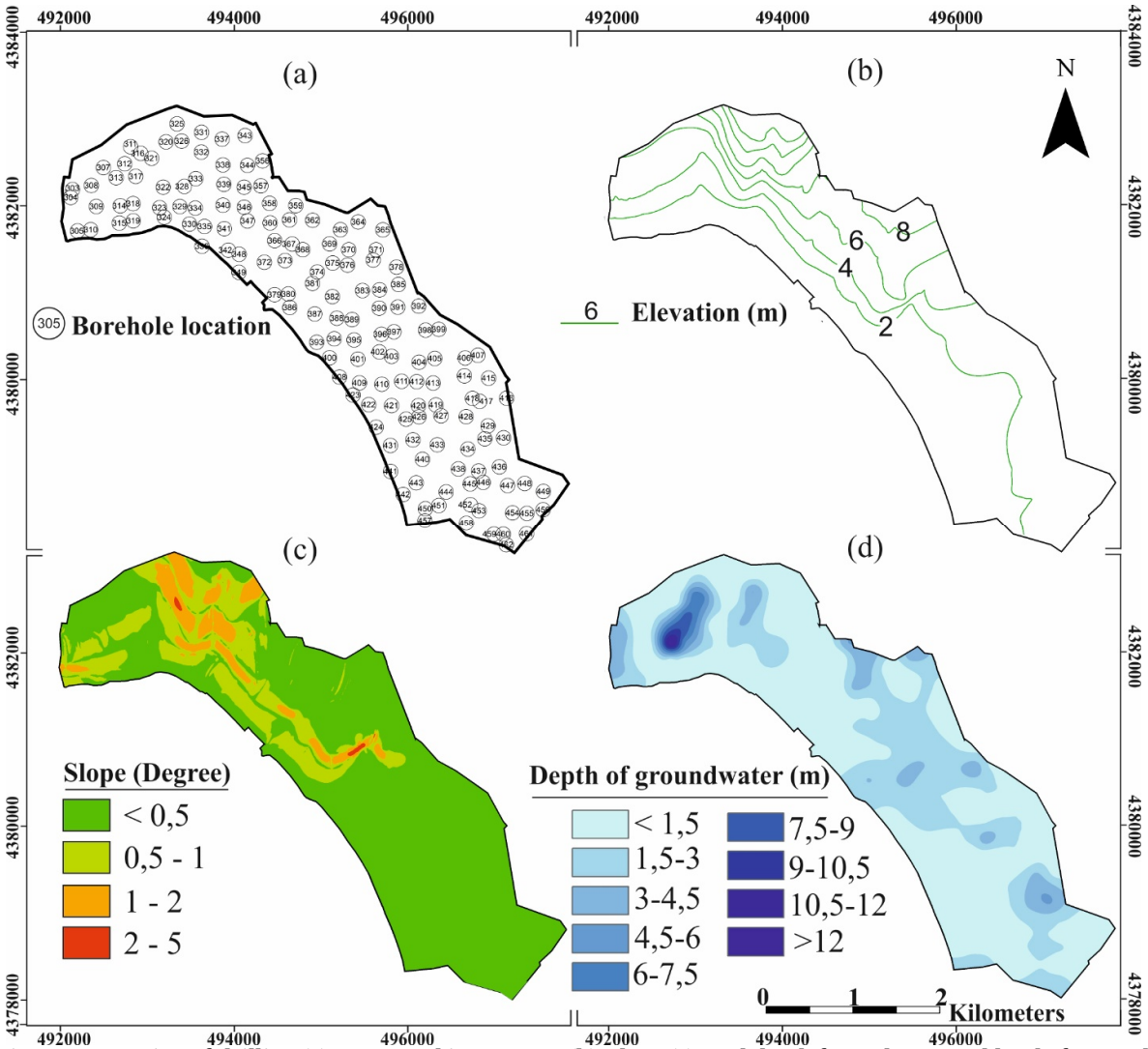

Figure 2. Location of drilling (a), topographic contours (b), slope (c), and depth from the ground level of ground water table (d) in the studied area.

According to the results of the sieve analysis, the soil layers of the alluvium in the study area composed of three different soil types. These are sandy, silty clay (50% to 74% clay, 16% to 18% silt and 8% to 39% sand), gravelly, clayey, silty sand (12% to 40% clay plus silt, 55% to 60% sand, and 0% to 33% gravel) and sandy gravel with clay and silt (4% to 11% clay plus silt, 22% to 36% sand, and 53% to 74% gravel) (Figure 3). The spatial distributions of these soil groups at different depths were given in the Figures (4). It can be seen that 73.3 % to 86.7% of the entire area (about 9.882

km^2) has gravelly, clayey, silty sand. 0.3% to 0.6 % of the entire area has gravelly sandy, silty clay while 12.6% to 25.8% of the entire area has sandy gravel with clay and silt.

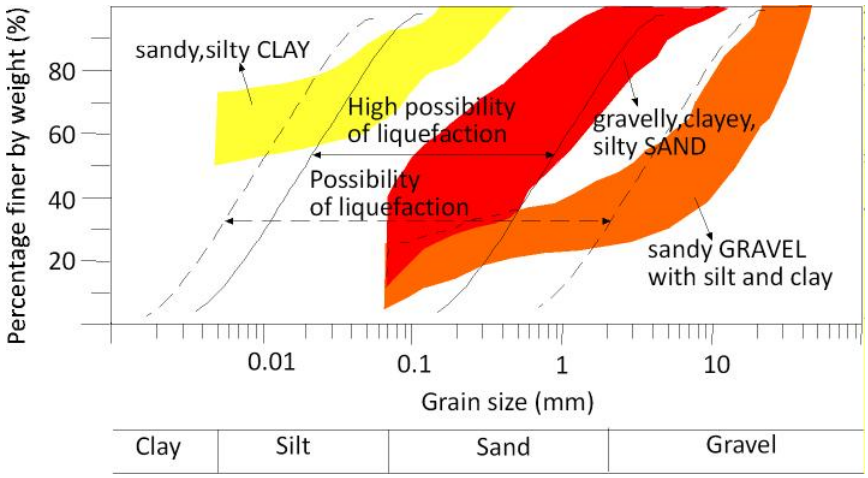

Figure 3. Graph of liquefaction potential level based on grain gradation [30] and the different soil types defined in the soil layers of the alluvium in the studied area.

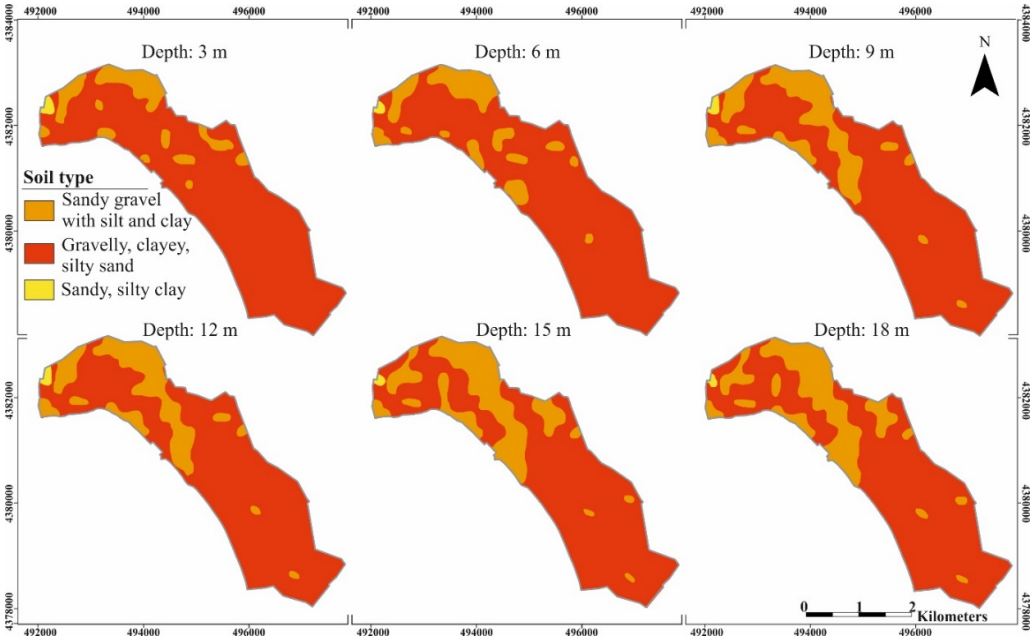

Figure 4. Spatial distribution of the soil types at the different depths

The spatial distribution of the corrected SPT-N value ($(N_1)_{60}$) at different depth were given in Figure 5. $(N_1)_{60}$ was determined for clear sand using Equation (1) [23].

$$(N_1)_{60} = C_R C_S C_B C_E C_N \quad (1)$$

where, C_S is non-standard sampler factor, C_R is rod length factor, C_E is hammer energy efficiency C_B is borehole diameter factor, and C_N is overburden factor. C_R, C_S, C_B and C_E values were obtained using the table given by Robertson and Wride (1998), [31]. The overburden correction factor (C_N) was calculated by using the Equation (2) [32].

$$C_N = \left(\frac{P_a}{\sigma'_V}\right)^{0.5} \quad (2)$$

where, Pa is 1 atm pressure (101 kPa) and σ'_v is vertical effective stress

.

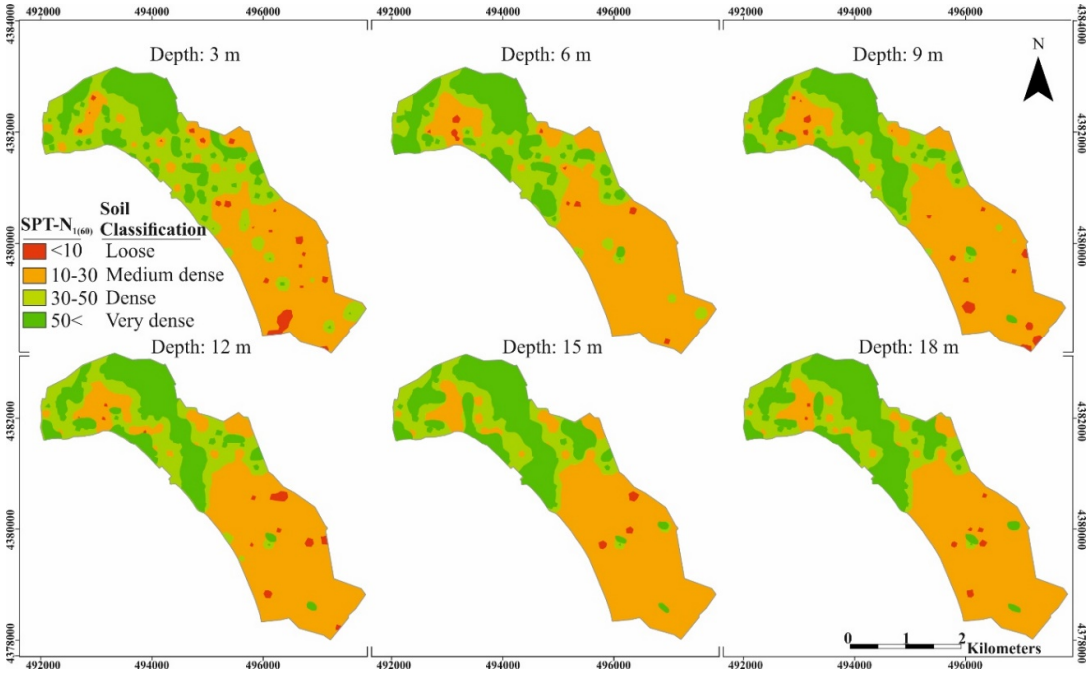

Figure 5. Spatial distribution of the value $(N_1)_{60}$, which is representing relative density of soil at different depths

4. Factor of Safety Against Liquefaction of Soil Layers

The models that follow Seed and Idriss (1971), [11] are based on the factor of safety against liquefaction (F_L) defined as the ratio of cyclic resistance ratio (CRR) over cyclic stress ratio (CSR) (Equation 3). Liquefaction of a soil is predicted to occur if F_L is less than or equal to 1.

$$F_L = \frac{CRR_{M=7.5}}{CSR_{M=7.5,\sigma'_v=1atm}} \quad (3)$$

CSR value corrected for M_w=7.5, and overburden pressures higher than 1 atm was calculated using the equation given in Youd *et al.*, (2001), [23], (Equation 4).

$$CSR_{M=7.5,\sigma'_v=1atm} = 0.65\frac{\sigma_v}{\sigma'_v}\frac{a_{max}}{g}r_d\frac{1}{MSF}\frac{1}{K_\sigma} \quad (4)$$

where σ_v is vertical total stress, σ'_v is vertical effective stress, g is gravity acceleration, rd is shear stress reduction factor, a_{max} is maximum horizontal ground surface acceleration, K_σ is the correction factor for effective overburden and MSF is the magnitude scaling factor.

The relation proposed by Seed and Idriss (1971), [11], which was approximated by Liao and Whitman (1986), [32] given following equation (Equation 5) was used in this study, where, z is depth from the ground surface.

$$r_d = \frac{(1.00 - 0.4113z^{0.5} + 0.0452z + 0.001753z^{1.5}}{(1.000 + 0.4177z^{0.5} + 0.05729z - 0.006205z^{1.5} + 0.001210z^2)} \quad (5)$$

The magnitude scaling factor (MSF) developed Idriss (1999) [33] was used in this study (Equation 6).

$$MSF = \frac{10^{2.24}}{M_w^{2.56}} \quad (6)$$

The term Kσ was computed as the formula given in Hynes and Olsen (1999), [35] (Equation 7).

$$K_\sigma = \left(\frac{\sigma'_V}{P_a}\right)^{(f-1)} \leq 1 \quad (7)$$

where Pa is 1 atm pressure (101 kPa) and σ'_v is vertica.l

In this study, the linear relationship for f suggested by Montgomery et al (2012), [35] was used (Equations 8, 9). C_d was taken as 46 by Idriss and Boulanger (2008), [36].

$$f = 1 - \left(\frac{D_R}{2}\right) \quad 0.6 \le f \le 0.8 \tag{8}$$

$$D_R = \sqrt{\frac{(N_1)_{60,CS}}{C_d}} \tag{9}$$

To find the peak ground acceleration, a_{max}, at the drill point, the short-period map spectral acceleration coefficient (Ss), and, the local soil coefficient, F_S, given depending on the soil type (Table 1) are used [28], (Equation 10).

$$a_{max}=0.4\ S_{DS} \tag{10a}$$

$$S_{DS}=S_S\ F_S \tag{10b}$$

where S_{DS} is the short-period spectral acceleration coefficient, S_S is the short-period map spectral acceleration coefficient. S_S was taken from Turkish Earthquake Hazard Maps, accessed through the website www.tdth.afad.gov.tr. a_{max} is the peak ground acceleration. F_S is local soil coefficient for short period zone (Table 1), [28].

The spatial distribution in the studied area of a_{max} is given at Figure 6.

Table 1. Local soil coefficient for short period zone [28].

Soil class	Soil type	$(N_{60})_{30}$	Local soil coefficient for short period zone (F_S)					
			$S_S \le 0.25$	$S_S=0.5$	$S_S=0.75$	$S_S=1$	$S_S=1.25$	$S_S \ge 1.5$
ZC	Very dense sand, gravel, and hard clay layers or weak jointed rocks	>50	1.3	1.3	1.2	1.2	1.2	1.2
ZD	Medium dense-dense sand, gravel or very hard class layers	15-50	1.6	1.4	1.2	1.1	1.0	1.0
ZE	Loose sand, gravel or soft-stiff clay layers or profiles with a soft clay layer thicker than 3 m in total providing plasticity index >20 and water content > 40%	<15	2.4	1.7	1.3	1.1	0.9	0.8

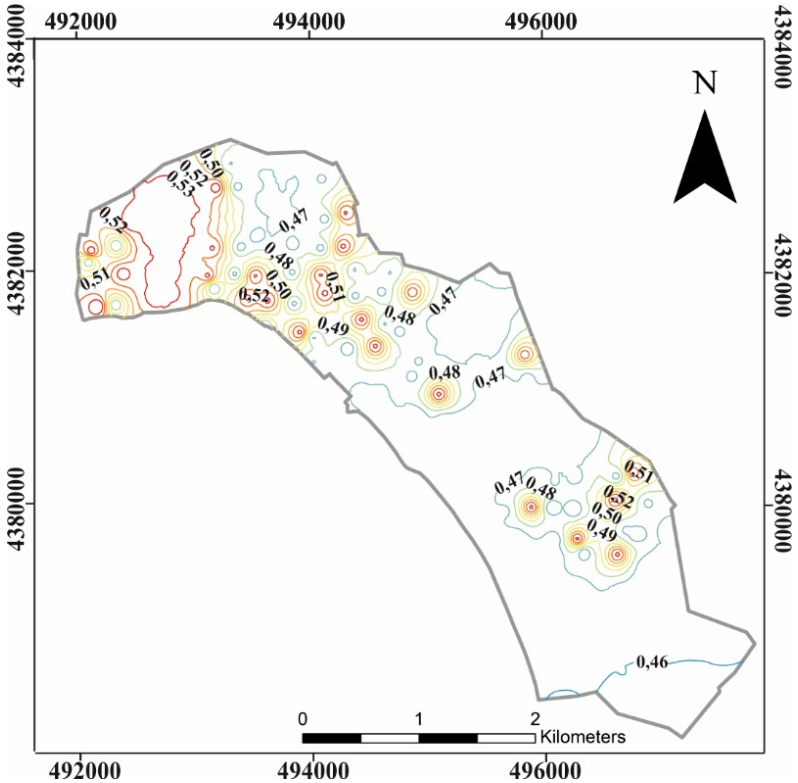

Figure 6. Spatial distribution in the studied area of the ratio of the peak ground acceleration/ ground acceleration

In the present study, the CRR value for an earthquake having moment magnitude of M_w = 7.5 was computed based on $(N_1)_{60CS}$ by using the following expression (Youd *et al.*, (2001), [23], (Equation 11a). The fines content correction, initially developed by Seed et al., (1985), [37] was applied for the correction of $(N_1)_{60}$ to an equivalent clean sand value using following equations (Equation 11b-h).

$$CRR_{7.5} = \frac{1}{34-(N_1)60cs} + \frac{(N_1)60cs}{135} + \frac{50}{[10(N_1)60cs + 45]^2} - \frac{1}{200} \quad (11a)$$

$$(N_1)_{60cs} = \alpha + \beta\,(N1)_{60} \quad (11b)$$

α=0 (for FC $\lesssim$ 5%) (11c)

$$\alpha = \exp\left[1.76 - \left(\frac{190}{IFCTO^2}\right)\right] \quad \text{(for 5\% < FC } \lesssim \text{ 35\%)} \quad (11d)$$

α=5 (for FC > 35%) (11e)

β= 1 (for FC $\lesssim$ 5%) (11f)

$$\beta = \left[0.99 + \frac{FC^{1.5}}{1000}\right] \quad \text{(for 5\% < FC } \lesssim \text{ 35\%)} \quad (11g)$$

β=1.2 (for FC > 35%) (11h)

where $(N_1)_{60}$ is corrected SPT-N value for overburden factor, rod length factor, non-standard sampler factor, borehole diameter factor, and overburden correction factor, FC is fine grained content.

The spatial distributions of the safety factor against liquefaction of soil layer at different depths were given in (Figure 7).

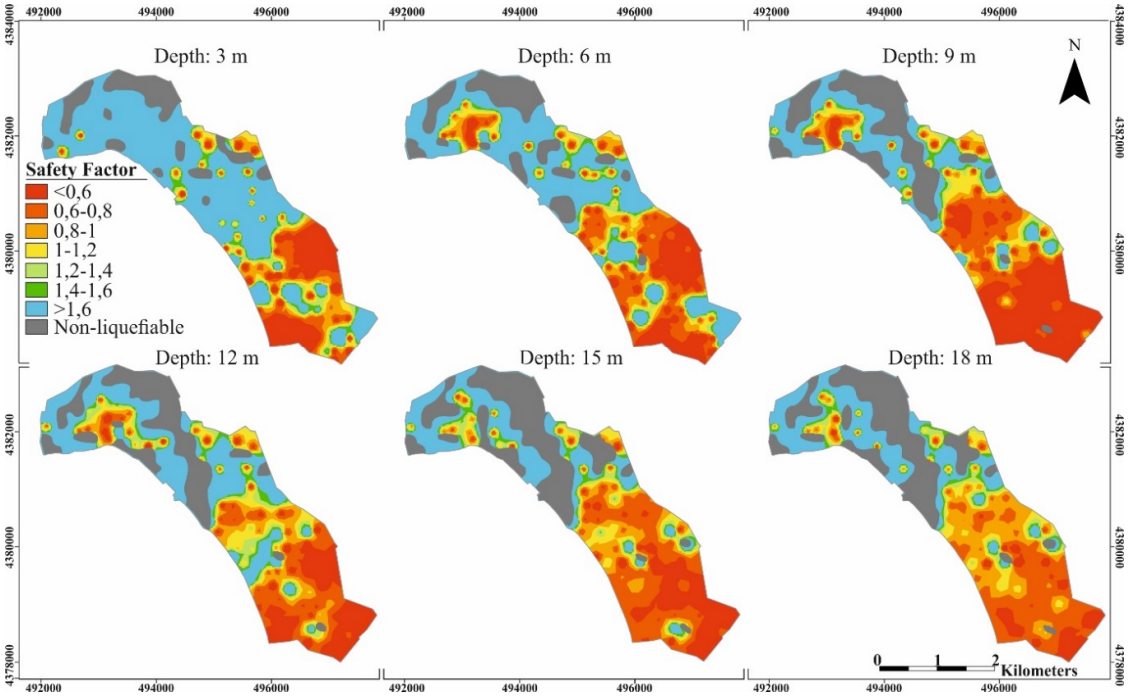

Figure 7. The spatial distributions of the safety factor against to liquefaction of soil layer at different depths

5. Liquefaction Potential Index Map and Liquefaction Severity Index Map

The factor of safety against liquefaction (F_L) can be used to predict that a soil layer can either liquefy or not liquefy, but not degrees of severity. The effect of liquefaction of a soil layer on possible damage to engineering structures depends on the thickness, depth and liquefaction severity of the liquefiable soil layer. To overcome these limitations of F_L, Iwasaki *et al.*, (1982), [38], defined the Liquefaction Potential Index (L_I) used to estimate the liquefaction damage risk (Equation 12). Then Sonmez (2003), [24] modified the equation suggested by Iwasaki *et al.*, (1982), [38]. In the present study, the Liquefaction Potential Index (L_I) was calculated the equations given in Sonmez (2003), [24] (Equation12).

$$L_I = \int_0^{20m} F(z)W(z)dz \quad (12a)$$

$$F(z) = 1 - F_L \text{ for } F_L \leq 0.95,$$

$$F(z) = 2x10^6 e^{-18.427F_L} \text{ for } 0.95 < F_L \leq 1.2 \quad (12b)$$

$$F(z) = 0 \text{ for } F_L < 1.2$$

$$W(z) = 10 - 0.5z \text{ for } z \leq 20m$$

$$W(z) = 0 \text{ for } z > 20m \quad (12c)$$

The spatial distribution of LPI obtained was given in Figure 8a.

Chen and Juang (2000), [39] and Lee *et al.*, (2003), [40] replaced the F(z) term of the L_I index with the probability of liquefaction for soil layer (P_L) (Juang *et al.*, 2003), [29] and also re-named L_I as Liquefaction Risk Index (I_R). Sonmez and Gokceoğlu (2005), [25] indicated that I_R calculation would give the soil profile its sensitivity to liquefaction and did not fully meet the risk term. For this, they suggest the use of Liquefaction Severity Index (I_R) which is proposed by Youd and Perkins (1987) [41]. The Liquefaction Severity Index modified by Sonmez and Gokceoğlu (2005), [25] was calculated using the following equations (Equation 13).

$$L_s = \int_0^{20} P_L(z)W(z)dz \quad (13a)$$

$$P_L(z) = \frac{1}{1 + (\frac{FL}{0.96})^{4.5}} \text{ for } F_L \leq 1.411 \quad (13b)$$

$$P_L(z) = 0 \text{ for } F_L > 1.411 \quad (13c)$$

where, the term of W(z) is as same as those in Equation 12c.

The spatial distribution of the Liquefaction Severity Index in the studied area was given following (Figure 8b).

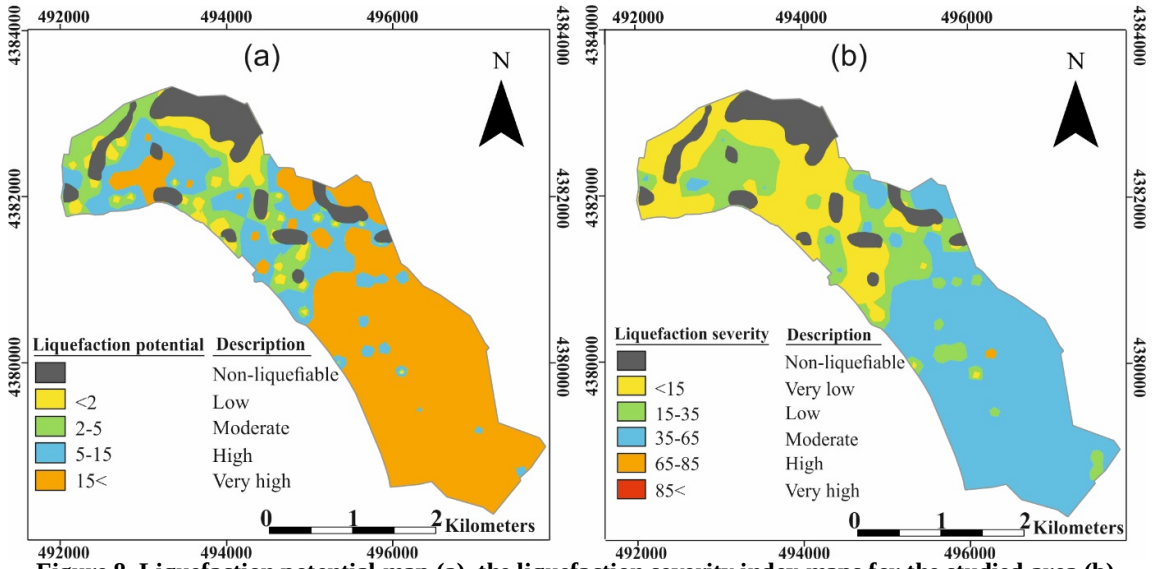

Figure 8. Liquefaction potential map (a), the liquefaction severity index maps for the studied area (b)

6. Conclusions

Balikesir province Akcay district (Biga Peninsula, South Marmara Region, Turkey), the studied area is located on the southern branch of the NAFZ in where some earthquake occurred in the instrumental period which caused some significant damages. Edremitt Fault Zone is 5.8 km

away from the study area and also Havran-Balikesir Fault Zone is 9.1 km away. In this study, topography, depth of groundwater table and soil characteristics of the said area were investigated in terms of susceptibility to liquefaction. The slope of 98 % of the study area having less than 2 degrees. Approximately 63.6 % of the study area has GWT depths >1.5 m, 13.4 % has GWT depths between 1.5 and 3.0 m, 11.7% have GWT depths between 3.0 and 4.5 m. and 9.5 % has GWT depths between 4.5 and 12 m. As it can be seen, in a very small area of the studied area that is less than 2 % of the studied area, groundwater table depth is greater than 12 m. The maps representing the spatial distributions of the soil groups, and corrected SPT-N value at 3 m, 6 m, 9 m, 12m, 15 m and depths were prepared. 73.3 % to 86.7% of the entire area (about 9.882 km^2) has gravelly, clayey, silty sand. 0.3% to 0.6 % of the entire area has gravelly sandy, silty clay while 12.6% to 25.8% of the entire area has sandy gravel with clay and silt. According to corrected SPT-N values, <3% of the entire area at different depth has loose soil, 46.7 % to 56.3 % of the entire area has medium dense soil, 17.2% to 30.5 % of the entire area has dense soil and 20.7% to 56.3% of the entire area has very dense soil. In addition, the spatial distributions of the factor of safety against liquefaction of soil layers (F_L) at 3m, 6m, 9 m, 12m, 15 m and 18 m depths were prepared. At these different depths, 19.3% to 39.8 % of the entire area has F_L value <0.8 6.1% to 15.2 % of the entire area has F_L value between 0.8 and 1.0, 4.9% to 7.7 % of the entire area has F_L value between 1.0 and 1.2, 25.0% to 57.5 % of the entire area has F_L value >1.2, and 12.3 % to 26.1 % of the entire area has none-liquefiable soil.

After the safety factor against liquefaction of soil layers defined in the said boring logs were calculated using the simplified method, the liquefaction potential index of soil profile in the location of boring were obtained and the liquefaction potential map was produced. It can see in the liquefaction potential map that 5.8% of the study area has low liquefaction potential, 10.7% medium liquefaction potential, 18.3% high liquefaction potential, and 53.8% very high liquefaction potential. The rate of the area where liquefaction is not expected is 11.4%. In addition, the probability of liquefaction for soil layer were calculated then the liquefaction severity index map for the study area was obtained. According to the liquefaction severity index map, 22.7% of the study area has very low liquefaction severity, 17.1% low liquefaction severity, 47.7% moderate liquefaction severity, and 1.1% high liquefaction severity and 11.4% of the studied area has none-liquefiable soil.

These maps prepared for the study area can be used in urban planning and to take precautions against the hazard of liquefaction. Especially in areas with high and very high liquefaction potential, groundwater level should be lowered and soil improvement should be done. In places where these cannot be done, buildings such as schools, places of worship, hospitals should be evacuated and new settlements should not be allowed.

References

[1]. Terzaghi K and Peck, RB (1948) *Soil Mechanics in Engineering Practice. John Wiley*.

[2]. ElGhoraiby MA, Park H and Manzar MT (2020) Stress-strain behavior and liquefaction strength characteristics of Ottawa F65 sand. *Soil Dynamics and Earthquake Engineering 138*, 106292.

[3]. Ishihara K and Koga Y (1981) Case studies of liquefaction in the 1964 Niigata Eartquake, *Soil snd Foundation*, 21(3):34-52.

[4]. Seed RB, Dickenson SE and Idriss IM (1991) Principal geotechnical aspects of the 1989 Loma Prieta earthquake. Soils and Foundations, *Japanese Society of Soil Mechanics and Foundation Engineering* 31(1):1-26.

[5]. Tanaka Y (2000) The 1995 Great Hanshin earthquake and liquefaction damages at reclaimed lands In Kobe Por. *International Society of Offshore and Polar Engineers* 10(1), 1-9, ISOPE-00-10-1-064.

[6]. Hwang JH, Yang CW and Chen CH (2003) Investigations on soil liquefaction during the Chi-Chi earthquake, *Soils and Foundations 43(6)*, 107-123. DOI: 10.3208/sandf.43.6-107.

[7]. Bray JD, Sancio RB, Durgunoglu T, Onalp A, Youd TL, Stewart JP, Seed RB, Cetin OK, Bol E, Batuary MB, Christensen C, Karadayilar T (2004) Subsurface characterization at ground failure sites in Adapazari, Turkey. *J Geotech Geoenviron Eng* 130(7):673 685.

[8]. Quigley MC, Bastin S and Bradley BA (2013) Recurrent liquefaction in Christchurch, New Zealand, during the Canterbury earthquake sequence. *Geology* 41(4):419–422.

[9]. Orense RP, Pender MJ and Wotherspoon LM (2012) Analysis of soil liquefaction during the Recent Canterbury (New Zealand) earthquakes. *Geotechnical Engineering Journal of the SEAGS & AGSSEA* 43(2), 8-17, ISSN 0046-5828.

[10]. Seed HB, Tokimatsu K, Harder LF Jr. and Chung, R (1984). The influence of SPT procedures in soil liquefaction resistance evaluations. Earthquake Engineering Research Center, *University of California, Berkeley, Report No. UCB/EERC-84/15, 50 pp*.

[11]. Seed HB and Idriss IM (1971) Simplified procedure for evaluating soil liquefaction potential, *Journal of the Soil Mechanics and Foundations Division ASCE* 97 (SM9, Proc. Paper 8371) 1249-1273.

[12]. Anon (2016) State of the art and practice in the assessment of earthquake-ınduced soil liquefaction and ıts consequences. A report of The National Academies of Sciences, Engineering, Medicine, *The National Academies Press, Washington*, DC, pp.297.

[13]. Dobry R and T Abdoun (2011) An investigation into why liquefaction charts work: A necessary step toward integrating the states of art and practice. *Pp. 1344 in Proceedings of the 5th International Conference on Earthquake Geotechnical Engineering*, 10-13 January, Santiago, Chile. Ishihara Lecture.

[14]. Kayabali K, Yilmaz P, Fener M, Akturk O and Habibzada F (2018) Assessment of soil liquefaction using the energy approach. *Bulletin of the Mineral Research and Exploration* 156:193-204.

[15]. Hakam A, Ismail FA and Fauzan F (2016) Liquefaction potential assessment based on laboratory test. *International Journal of Geomate* 11(26):2553-2557.

[16]. Rapti I (2016) Numerical modeling of liquefaction-induced failure of geostructures subjected to earthquakes. Construction hydraulique. *Université Paris-Saclay - CentraleSupélec, English. ffNNT : 2016SACLC025ff*. fftel-01329628.

[17]. Ekinci YL and Yigitbas E (2012) A geophysical approach to the igneous rocks in the Biga Peninsula (NW Turkey) based on airborne magnetic anomalies: *geological implications. Geodinamica Acta*, 25 (3–4), 267–285.

[18]. Sozbilir H, Ozkaymak C, Uzel B and Sumer O (2018) Criteria for surface rupture microzonation of active faults for earthquake hazards in urban areas, N. Handbook of research on trends and digital advances in engineering geology, 765 pages, *IGI Globa*l, DOI: 10.4018/978-1-5225-2709-1.

[19]. Alsan E, Tezuçan L andBåth M (1976) An earthquake catalogue for Turkey for the interval 1913–1970 *Tectonophysics* 31 (1-2), T13-T19

[20]. Sozbilir H, Sumer O, Ozkaymak C, Uzel B, Guler T and Eski S (2016a) Kinematic analysis and paleoseismology of the Edremit Fault Zone: evidence for past earthquakes in the southern branch of the North Anatolian Fault Zone, Biga Peninsula, NW Turkey. *Geodinamica Acta*, 28(4): 273–294.

[21], Sozbilir H, Ozkaymak C, Uzel B, Sumer O, Eski S and Tepe C (2016b) Paleoseismology of the Havran-Balıkesir Fault Zone: Evidence for past earthquakes in the strike- slip-dominated contractional deformation along the southern branches of the North Anatolian fault in northwest Turkey. *Geodinamica Acta*, *28*(4), 254–272.

[22]. Uzel B. (2016) Field evidence for normal fault linkage and relay ramp evolution: the Kırkağaç Fault Zone, western Anatolia (Turkey). *Geodinamica Acta*, 28, 311-327.

[23]. Youd TL, Idriss IM, Andrus RD, Arango I, Castro G, Christian JT, Dobry R, Finn WDL, Harder LF, Jr, Hynes ME, Ishihara K, Koester JP, Liao SSC, Marcuson WF, Martin GR, Mitchell JK, Moriwaki Y, Power MS, Robertson PK, Seed RB and Stokoe KH (2001) Liquefaction resistance of soils: summary report from the 1996 NCEER and 1998 NCEERINSF workshops on evaluation of liquefaction resistance of soils, *J Geotech Geoenviron Eng* 127(10):817-833.

[24]. Sonmez H (2003) Modification of the liquefaction potential index and liquefaction susceptibility mapping for a liquefaction-prone area (Inegol, Turkey). *Environ Geol* 44(7):862–871

[25]. Sonmez H and Gokceoglu C (2005) A liquefaction severity index suggested for engineering practice. *Environ Geol* 48(1):81–91.

[26]. Analysis Engineering Drilling Mining Construction Industry and Trade Limited Company (2017) The Micro-zoning Study Report based on the Zoning Plan of the Area, 4906.79-hectare, in Balikesir Province Edremit District, *January 2017. İstanbul, Turkey* (in Turkish).

[27]. American Society for Testing and Materials (ASTM) D2487-06 (2010) Standard Practice for Classification of Soils for Engineering Purposes (Unified Soil Classification System). *West Conshohocken*, PA, 2006.

[28]. TBEC (2018) Turkish Building Earthquake Code 2018, T.C. *The Official Journal: Ankara*, Turkey.

[29]. Juang CH, Yuan H, Lee DH and Lin PS (2003) A simplified CPT-based method for evaluating liquefaction potential of soils. *J Geotech Geoenviron Eng* 129(1):66–80.

[30]. Tsuchida H (1970) Prediction and countermeasure against liquefaction in sand deposits Sem. of the Port and *Harbor Research Institute*.

[31]. Robertson, P. & Wride, C.E.. (1997). Cyclic liquefaction and its evaluation based on SPT and CPT. Proc. NCEER Work-shop on Evaluation of Liquefaction Resistance of Soils. Report NCEER-97-0022, *National Center for Earthquake Engineering Research*, SUNY Buffalo, NY.

[32]. Liao S and Whitman RV (1986) Overburden correction factors for SPT in sand. *J Geotech Eng* 112(3):373–7.

[33]. Idriss IM (1999) An update of the Seed-Idriss simplified procedure for evaluating liquefaction potential, Presentation notes for Transportation Research Board Workshop on New Approaches to Liquefaction Analysis, Washington, D.C.

[34]. Hynes ME and Olsen RS (1999) Influence of confining stress on liquefaction resistance. Proc., *Int. Workshop on Phys. And Mech. Of Soil Liquefaction*, Balkema, Rotterdam, The Netherlands, 145-152.

[35]. Montgomery J, Boulanger RW and Harder LF (2012) Examination of the K_σ overburden correction factor on liquefaction resistance. Report No. UCD/CGM-12-02, Center for Geotechnical Modeling Department of Civil and Environmental Engineering University of California, Davis, California, pp.42.

[36]. Idriss IM and Boulanger RW (2008) Soil liquefaction during earthquakes, Monograph MNO-12, *Earthquake Engineering Research Institute*, Oakland, CA.

[37]. Seed HB, Tokimatsu K, Harder LF Jr and Chung R (1985) Influence of SPT procedures in soil liquefaction resistance evaluations, *J Geotech Eng* 111(12):1425-1445.

[38]. Iwasaki T, Tokida K, Tatsuoka F, Watanabe S, Yasuda S and Sato H (1982) Microzonation for soil liquefaction potential using simplified methods. *3rd International Earthquake Microzonation Conf* 1319–1330.

[39]. Chen CJ and Juang CH (2000) Calibration of SPT- and CPT-based liquefaction evaluation methods. Innovations Applications in Geotechnical Site Characterization, Mayne, P. and Hryciw, R., Eds., *Geotechnical Special Publication* No. 97, ASCE, New York, 49−64.

[40]. Lee D-H, Ku C-S and Yuan H (2003) A study of the liquefaction risk potential at Yuanlin, Taiwan. *Eng Geology* Elsevier, 71:97–117.

[41]. Youd TL, Perkins DM (1987) Mapping of liquefaction severity index. *J Geotechnical Eng* ASCE, 113; 1987. p. 1374–92.

حساسیت روانگرایی خاک منطقه مسکونی آکچای (شبه جزیره بیگا، ترکیه) نزدیک به منطقه گسل آناتولی شمالی

سنر سریان[1]، پیجوش ساموییی[2]، عثمان سامد اوزکان[3]، سامت بربر[1]، سوله تودس[4]، هاکان السی[5]*، و نورچیان سریان[6]

1. گروه مهندسی زمین شناسی، دانشگاه بالیکسیر، بالیکسیر، ترکیه

2. گروه مهندسی عمران، NIT Patna، Patna، Bihar، هند

3. دانشکده تحصیلات تکمیلی علوم طبیعی و کاربردی، دانشگاه بالیکسیر، بالیکسیر، ترکیه

4. گروه برنامه ریزی شهری و منطقه‌ای، دانشکده معماری دانشگاه گازی، آنکارا ترکیه

5. مدرسه حرفه‌ای Torbalı ، دانشگاه Dokuz Eylul ، ازمیر، ترکیه

6. گروه معدن و استخراج مواد معدنی، مدرسه حرفه‌ای بالیکسیر، دانشگاه بالیکسیر، بالیکسیر، ترکیه

ارسال 2023/05/18، پذیرش 2023/06/28

* نویسنده مسئول مکاتبات: hakan.elci@deu.edu.tr

چکیده:

استان بالیکسیر منطقه آکچای (شبه جزیره بیگا، منطقه مرمره جنوبی، ترکیه)؛ منطقه مورد مطالعه در شاخه جنوبی منطقه گسل آناتولی شمالی، جایی که زمین لرزه 1867 (Mw = 7.0) Edremit، 1919 Ayvalik-Sarmisakli (Mw = 7.0)، ادرمیت 1944 (Mw = 6.4) و 1953 Yenice (Mw) واقع شده است. زمین لرزه در دوره تاریخی و ابزاری رخ داده است. در منطقه مذکور به طور کلی سطح آب‌های زیرزمینی بالا بوده و خاک‌های شنی گسترده است. در این مطالعه، توپوگرافی، عمق سطح آب زیرزمینی و خصوصیات خاک منطقه مذکور از نظر حساسیت به روانگرایی بررسی شد. علاوه بر این، ضریب ایمنی در برابر روانگرایی (FL) برای لایه‌های خاک با استفاده از روش ساده بر اساس مقادیر SPT-N تعیین شد. سپس توزیع فضایی ضریب ایمنی در عمق های 3 متر، 6 متر، 9 متر، 12 متر، 15 متر و 18 متر به دست آمد. با در نظر گرفتن مقادیر FL به‌دست‌آمده، شاخص پتانسیل روان‌گرایی و شاخص شدت روان‌گرایی پروفیل خاک در محل حفاری محاسبه شد، سپس توزیع‌های مکانی این شاخص‌ها به‌دست آمد. بر اساس نقشه‌های به دست آمده، 5,8 درصد از منطقه مورد مطالعه دارای پتانسیل روانگرایی کم، 10,7 درصد پتانسیل روانگرایی متوسط، 18,3 درصد پتانسیل روانگرایی بالا و 53,8 درصد پتانسیل روانگرایی بسیار بالا و 22,7 درصد از منطقه مورد مطالعه دارای شدت روانگرایی بسیار پایین است. 17,1 درصد شدت روانگرایی کم، 47,7 درصد شدت روانگرایی متوسط و 1,1 درصد شدت روانگرایی بالا و 11,4 درصد از منطقه مورد مطالعه دارای خاک غیر روانگرایی است.

کلمات کلیدی: منطقه گسل آناتولی شمالی، روانگرایی خاک، شاخص پتانسیل روانگرایی، شاخص شدت روانگرایی.